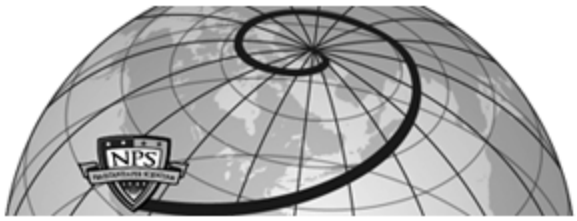

# UNITED STATES
# NAVAL POSTGRADUATE SCHOOL

## THESIS

ABSOLUTE NEUTRON FLUX

OF THE AGN-201 REACTOR

****

Roger Edison Perry, Jr.

# ABSOLUTE NEUTRON FLUX OF THE AGN-201 REACTOR

by

Roger Edison Perry, Jr.
Lieutenant Commander, United States Navy

Submitted in partial fulfillment of
the requirements for the degree of

MASTER OF SCIENCE

IN

PHYSICS

United States Naval Postgraduate School
Monterey, California

1964

ABSOLUTE NEUTRON FLUX

OF THE AGN-201 REACTOR

by

Roger Edison Perry, Jr.

This work is accepted as fulfilling

the thesis requirement for the degree of

MASTER OF SCIENCE

IN

PHYSICS

from the

United States Naval Postgraduate School

William W. Havens

Faculty Advisor

Austin R. Frey

Chairman

Department of Physics

Approved: D. E. Dimell

Academic Dean

## ABSTRACT

Absolute total and thermal neutron flux of the U. S. Naval Postgraduate School's AGN-201 reactor was determined by neutron activation of thin gold foils. Foil activities were measured with a gamma-ray scintillation spectrometer, using methods designed to minimize the effect of changes in spectrometer gain. Flux values were calculated for nominal power levels of 0.1 watt and 1, 10, 100, and 750 watts. Methods and results are compared with those of previous investigations. The flux level was found to be a linear function of power within this range; total and thermal average fluxes were determined to be respectively $6.64 \times 10^7$ and $5.41 \times 10^7$ neutrons per square centimeter per second per watt.

TABLE OF CONTENTS

## LIST OF ILLUSTRATIONS

1. Introduction.

Activation and decay measurement of gold foils has become a standard technique for determining reactor neutron flux. For the U. S. Naval Postgraduate School's AGN-201 reactor, this method has been used by Kelly and Clements (10) to determine the absolute thermal flux at 0.1 watt, by Ferguson and Harvey (6) to determine relative flux and flux distribution at several power levels, and by Copeland and Reasonover (4) to determine the flux perturbation caused by the presence of the foil. In the present investigation, the absolute flux was measured at several power levels, from 0.1 watt to 750 watts.

For measuring the absolute disintegration rate of the irradiated foil, several methods have been developed. Those which depend on beta-counting require the least special equipment, but they involve the corrections and difficulties associated with absolute beta measurements. It is possible to compare the activation induced by the reactor with that from a standard neutron source; this technique is also easy to apply, but the results are only as good as the accuracy to which the neutron density and energy distribution of the source are known. For speed and overall accuracy, gamma-ray spectrometry presents several advantages, and spectrometry was the technique used in the present investigation. The characteristics of scintillation spectrometers require precautions to be taken against drift of the photomultiplier tube and of the counting circuits themselves; this drift occurs from several causes, and it is not always apparent from the results of a short series of counts. In order to compensate for the effects of drift, a somewhat novel procedure was used for determining the parameters of the principal gold photopeak, that at 0.411 MEV.

2. Experimental procedure.

Thin circular gold foils, with nominal dimensions of 0.5" x 0.0005" and a mass of about 30 mg, were weighed to the nearest 0.5 mg and were rapidly inserted into the glory-hole of the reactor after it had been stabilized at the desired power. The foils were located at the center of the core to an estimated accuracy of $\pm$ 1 mm, and insertion and removal times were controlled to $\pm$ 1 second. For each run, the sample holder also contained an indium foil monitor, which was located in the graphite reflector 9" from core center. This location was chosen to minimize flux depression from the indium, while still exposing it to a significant neutron population. In addition, the characteristics of the reactor are such that the flux distribution in the reflector is relatively constant compared to that at the edges of the core; thus any position error would have minimum effect. The results of Ferguson and Harvey showed that at the location of the monitor foil the epithermal flux is negligible, so that no correction for fast flux was required; this conclusion may not be valid for power levels above 100 watts.

Foils were irradiated at 0.1, 1, 10, 100, and 750 watts. Although the reactor can be brought to 1000 watts for a short time, it was difficult to maintain accurate control as the sample holder was inserted and to reproduce conditions exactly for duplicate runs. Insertion of the sample holder causes an unavoidable change in reactivity, which requires adjustment of the control rods, and at high power levels the uncertainty in the neutron flux to which the foil was exposed and in the timing becomes greater. To minimize these errors would have required an exposure time that would have produced, at 1000 watts, an unacceptably high level of activity, because of the length of time the samples would have had to decay before counting. For these reasons, 750 watts was the maximum

level at which measurements were attempted.

Duplicate runs were made on all samples. Irradiation times were the same for both runs at each power level, except that during the first activation at 0.1w a line voltage transient caused an undesired scram which interrupted the run. The irradiation time given is corrected for sample decay during the interruption. The exposure times for the various runs were:

0.1 watt -- 477.7 minutes (corrected) and 534 minutes

1 watt -- 60 minutes

10 watts -- 30 minutes

100 watts -- 10 minutes

750 watts -- 5 minutes

Several factors affected the choice of irradiation time. A minimum of ten minutes was considered desirable, in order to minimize the relative error caused by insertion and removal times. For the lower powers, additional time was required to bring the activity to a level at which the photopeak maximum would be at least the several thousand counts per minute necessary to give a clear and sizable photopeak and to reduce the uncertainties produced by counting statistics and by background. On the other hand, to prevent coincidence losses in the spectrometer the maximum count was not allowed to rise above about 20,000 cpm; this meant that the 100 watt samples had to decay for about six days before being counted, and the effect of uncertainty in the accepted 2.7 day half-life of Au-198 could be significant. The 5-minute time chosen for the 750 watt run was a compromise between decay and timing errors.

Upon removal from the reactor, the indium and, when necessary, the gold foils were allowed to decay until their activities were at a suitable level for counting. The indium was counted in a standard G-M counter; the location of the foil in the counter was carefully reproduced for each run, but since only relative activity was required, no absorption or geometry corrections were applied. Two integrated 10-minute counts were taken of each indium foil. Coincidence and decay corrections were applied directly to the integrated count to determine foil activity; the method of determining the coincidence correction is given in Appendix I. In the higher-power runs, a significant (up to 1000 cpm) activity due to In-114 was observed. Since this isotope has a 49-day half-life, it was only necessary to allow each foil to decay for 24 hours; after this period the activity of In-116 was reduced by a factor of $10^8$, and the remaining activity was from In-114. The foil was then counted a second time, and the second count was subtracted from the first as "background".

Whether or not the activity of the gold was high enough to require additional decay time before counting, the first foil from each power level was allowed to remain in the spectrometer sample mount overnight before counting, in order to stabilize the photomultiplier tube as far as possible. The foil was placed on the "3cm" shelf of the mount, and the high voltage of the spectrometer was set at 1270 volts throughout; it has been determined that this combination gives good results. The gain and bias controls of the spectrometer were adjusted to give a usable peak, as discussed below. The 0.411 MEV photopeak was counted at least five times for each foil. Since the only information desired was the parameters of the photopeak, no attempt was made to determine the

entire spectrum, or to count more channels than were needed to ensure inclusion of the peak. The counts were corrected for foil decay before the photopeak area was computed; this approach permitted immediate, direct comparison of the results of duplicate runs. Decay-corrected peak count data are presented in Appendix II.

3. Spectrometer stability and drift.

Any variation in the overall gain of a spectrometer will appear as a drift or shift in the channel at which the photopeak maximum appears for gammas of a given energy. The variables involved have been discussed by Altekruse (1), Covell and Euler (5), and Cantarell (2), among others. Briefly, there are four primary causes of channel drift: (a) "fatigue", of the photomultiplier; (b) short-term gain changes in the photomultiplier, caused by temperature changes, high-voltage fluctuations, mechanical vibrations, etc.; (c) overall gain changes in the electronic circuitry, caused by tube and component aging; (d) short-term electronic changes caused by temperature and voltage transients. Previous investigators at this school apparently concluded that the spectrometer was "stable" if the photopeak maximum appeared in the same spectrometer channel on all runs; that this is too broad an assumption is shown by the fact that at the gain settings used by Copeland and Reasonover, a shift of one full 5-volt channel corresponds to a gamma energy change of 0.015 MEV, while in Kelly and Clements' work a 1-channel shift corresponds to 0.032 MEV of energy. Although a shift or drift of almost one channel was observed on one run during the present work, most of the shifts which occurred were of the order of a tenth of a channel width, and at the gain setting used, one channel corresponded to only 0.010 MEV. Although long-

term channel drift is not as serious in this type of work as it is in the analysis of unknown materials, there is still an observable effect, and rapid shifts caused by transients can completely invalidate a run. The result of a shift is to distort the apparent shape of the photopeak; if the drift is "down-channel", as most of it is, a progressively smaller fraction of the "actual" number of events appears in the count taken on each successive channel. If the area of the photopeak is then computed by the method given by Heath (7)(8), which involves fitting a curve to the points on the high side of the photopeak, the result indicates a narrower photopeak, hence a lower level of activation, than is actually present.* Similarly, an "up-channel" shift gives activation values which are too high. Because of the steep sides of the normal distribution curve which contains the photopeak, a rather slight shift in gain can cause a relatively large change in the computed area. Inspection of the data of the previous investigators shows that they did indeed encounter some drift, which they attempted to compensate by averaging the readings obtained on each channel from several counts. The validity of this procedure is questionable; it will be discussed below.

Of the causes of gain drift previously listed, the slow aging of electronic components was considered to be negligible over the hour or two required for each set of counts, although its effect could easily be observed

---

*The effect of the shift is to make the high side of the distribution curve appear steeper than it actually is. The error comes from the time required to count each channel; the true shape of the photopeak is unchanged, but it is moving to the left during the counting interval. This apparent steepening of the curve does not involve an increase in the resolution of the system, which is about 11 % at 0.411MEV.

over a period of months. Temperature, too, stayed fairly constant for any one counting period, and its effect on the electronic circuits was minimized in any case by leaving the spectrometer on, except for necessary repairs, throughout the period of this work. The situation with regard to electronic and photomultiplier transients was not so simple. That these transients did occur was not doubted; sharp changes in line voltage, for instance, if strong enough to scram the reactor, would certainly affect the spectrometer. In one case, an early difficulty with anomalous counts was resolved when it was noticed that the questionable counts were those taken just before and after each hour. The trouble was ascribed to the school's automatic clock-setting signal, whose 3600 cycle frequency could quite easily feed into the instrument, despite power supply regulation. Subsequent counts taken near the end of an hour were checked very carefully before being accepted.

The most important cause of channel drift is fatigue of the photomultiplier tube. Cantarell has shown that fatigue is caused by polarization of the dynodes after electron bombardment, which produces an "insulating" effect. The amount of fatigue is a function of temperature and high voltage, but more directly of count rate and gamma energy. A tube subjected to a given rate of scintillation events changes its gain over a period of hours; this gain change may be as high as 20%. The rate of gain change is logarithmic; in the present work, the effect of drift was minimized by leaving the first sample of each duplicate pair in the scintillator mount overnight. By the next day the tube was on the asymptotic portion of its fatigue curve, and the effect of the slight remaining drift was reduced by counting across the photopeak as fast

as possible for each run.* In view of the precautions observed, it is believed that the only significant distortion of the shape of recorded photopeaks was due to the fortuitous combination of the "vertical" random errors of counting statistics and "horizontal" random errors from the gain shifts caused by unpredictable and uncorrectible transients.

4. Photopeak parameter computations.

Even if the spectrometer were perfectly stable, the count recorded on each channel would be subject to a statistical probable error of the square root of the count. As has been mentioned, previous investigators have averaged successive counts on each channel, as one would do for total counts obtained with a G-M tube. Only a small change in system gain, however, will change count rates by several probable errors. Transient-induced gain shifts, rather than statistical variations, were in fact responsible for a majority of the differences between different counts of the same sample, as can be seen from examination of the data in Appendix II. When four points are taken on each of two readings, the statistical probability of all four shifting in the same direction is one in eight. As it happens, in over half of the cases observed all four channels shifted together, giving a strong indication that statistics alone was not causing the variation. (In evaluating these data, one must keep in mind that the first channel used is, in most cases, slightly below the photopeak maximum, whereas the last three are all above it. On a shift of the maximum to the left, the count

---

* The automatic readout feature of the spectrometer was not used, because recording a count manually is nearly twice as fast.

observed in the first channel will increase, while the other three will decrease.) If the peak shifts themselves were completely random, and if they took place at a random rate, simply taking the mean of enough different counts would compensate for shifts as well as for decay statistics. This simple approach was rejected for two reasons: (1) because of tube fatigue, there was a net overall drift to the left; (2) most of the shifts not attributable to tube fatigue, although they might drive the photopeak maximum in either direction, occurred at a rate corresponding to five or ten complete counts over the photopeak. To average these out would have required the recording of thirty or more counts of each sample, and since each complete count required about ten minutes, this approach was uneconomical.

For these reasons, it was decided to treat each count over the photopeak as a distinct event, compute the areas obtained individually, and average them at the end. By so doing, the effect of slow drift was made negligible, since it was well within statistical variations during the four or five minutes required to count four channels. A very fast shift, caused by a rapid transient, would give a curve whose computed maximum or area was so different from the remainder that it could be identified and discarded.

The standard method of computing the area under the photopeak is due to Heath. A normal distribution of events about the 0.411 MEV maximum is assumed; when this curve is plotted on a semi-logarithmic scale, the result is a parabola. In evaluating experimental data, observed counts of channels at and above the photopeak maximum are used in order to avoid distortion introduced by Compton scattering on the

low side of the peak. A parabola is fitted to the natural logs of these counts, and the parameters of the associated Gaussian curve are then determined. In the method of computation, however, the present procedure differed somewhat from that previously used. Kelly and Clements took several counts on each of three or four channels to determine their parabola and fitted the curve to the normalized average of their results. If each count over the photopeak is considered separately, taking only three points from each count does indeed give a set of perfect parabolas, but statistical variation makes them differ greatly from each other. Consequently, in the present work the spectrometer gain was adjusted so that the maximum point and high side of the photopeak covered at least four channels. A program was made up for the CDC 1604 computer which took the log functions, fitted a least-squares parabola to them, then gave the peak abscissa, peak ordinate, and area of the normal curve so derived. Because of the greater relative variation of the smaller counts, it was necessary to introduce a weighting factor. The weight of each count was made proportional to its square root; this procedure made use of the greater relative precision to be expected from the higher counts without completely swamping the smaller ones. If no weighting factor is applied, the statistical variation of the smaller counts causes the "tail to wag the dog", so to speak, and makes computed areas differ by an excessive amount.

The photopeak areas obtained for each count, their mean for each foil activation, and the standard deviation of the mean, are listed in Appendix III. The precision of results computed in this manner is about half that obtained from simple averaging of counts on each channel, but

one can at least feel confident that no systematic distortion of the photopeak is giving consistently high or low results.

5. Scintillation crystal efficiency.

The sample mount assembly used had been carefully constructed to give sample distances (for a thin mounting shelf) of 1, 2, 3, 5, and 10 cm from the face of the scintillation crystal, assuming that the crystal was snug against its can. Upon a recommendation from Mr. R. L. Heath, of the Phillips Petroleum Company, X-ray photographs were taken to check this assumption, and it was found to be incorrect. There is a gap, partially filled by what appears to be a spring spacer, of 9.0 mm between the 0.005" aluminum can and the face of the crystal (Figure 1). When this distance is added to the thickness of the mounting shelf, a sample in the "3 cm" position is actually 4.03 cm from the face of the crystal. Efficiencies previously used for this crystal and mount had been taken from Heath's standard catalogue and handbook of scintillation spectrometry (7)(8); they are on the order of 0.118, for a 3cm distance. The true value for 4.03 centimeters was computed by Heath (9) for this investigation; it is 0.0846.

6. Relative flux from indium monitor activation.

Relative flux levels derived from beta counts of the indium monitor foils, normalized to 1 watt, are plotted in Figure 2. Each point represents the average of two counts on each of two duplicate runs; deviations are too small to plot. As can be seen, from 0.1 to 100 watts the flux is linear with power to the precision of the measurements. No explanation is offered for the high values found at 750 watts; the small deviation obtained in independent measurements suggests that this is a true value

Crystal and sample mount

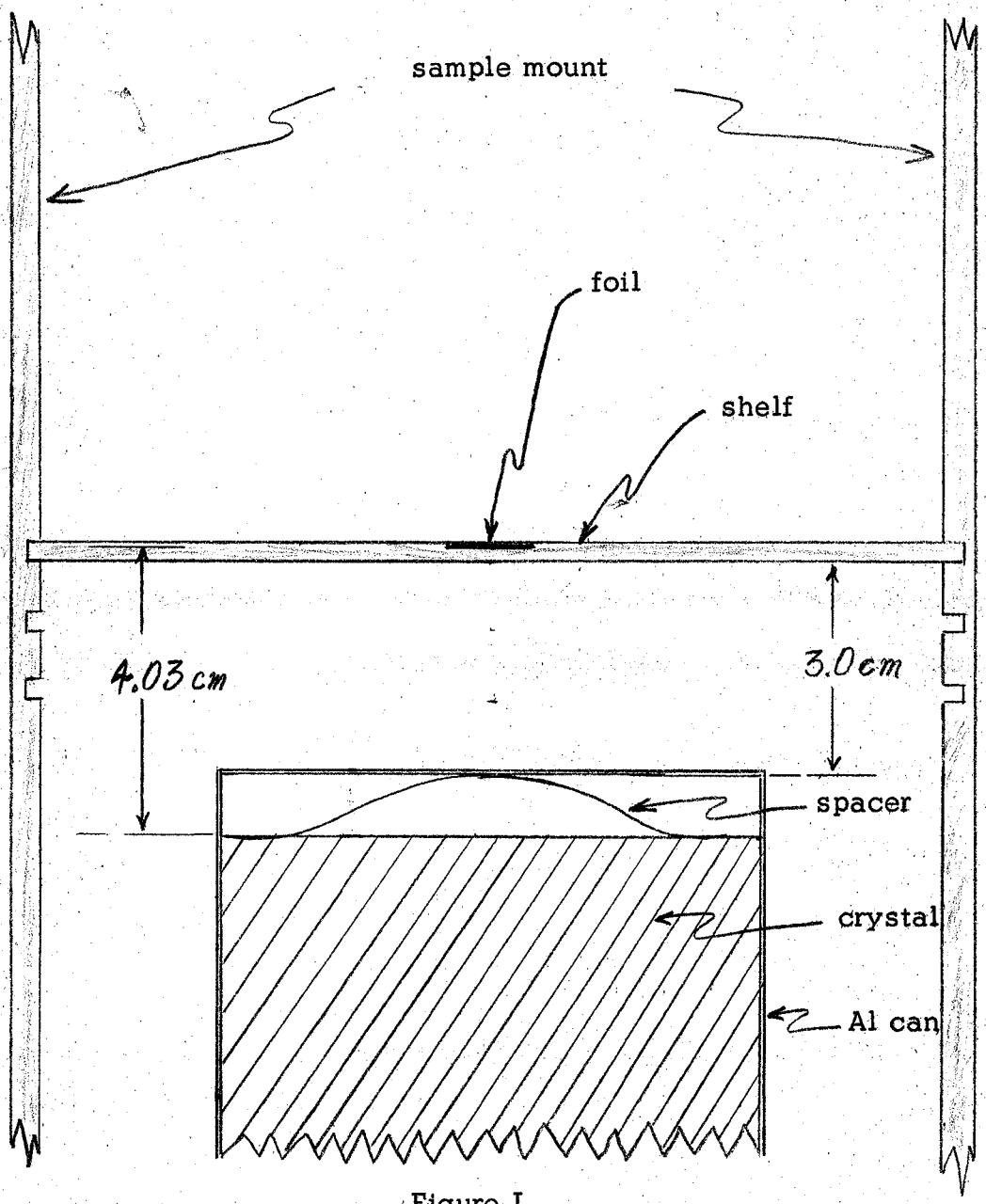


Figure I

Relative flux vs power level for indium monitor foils (normalized to 1 watt)

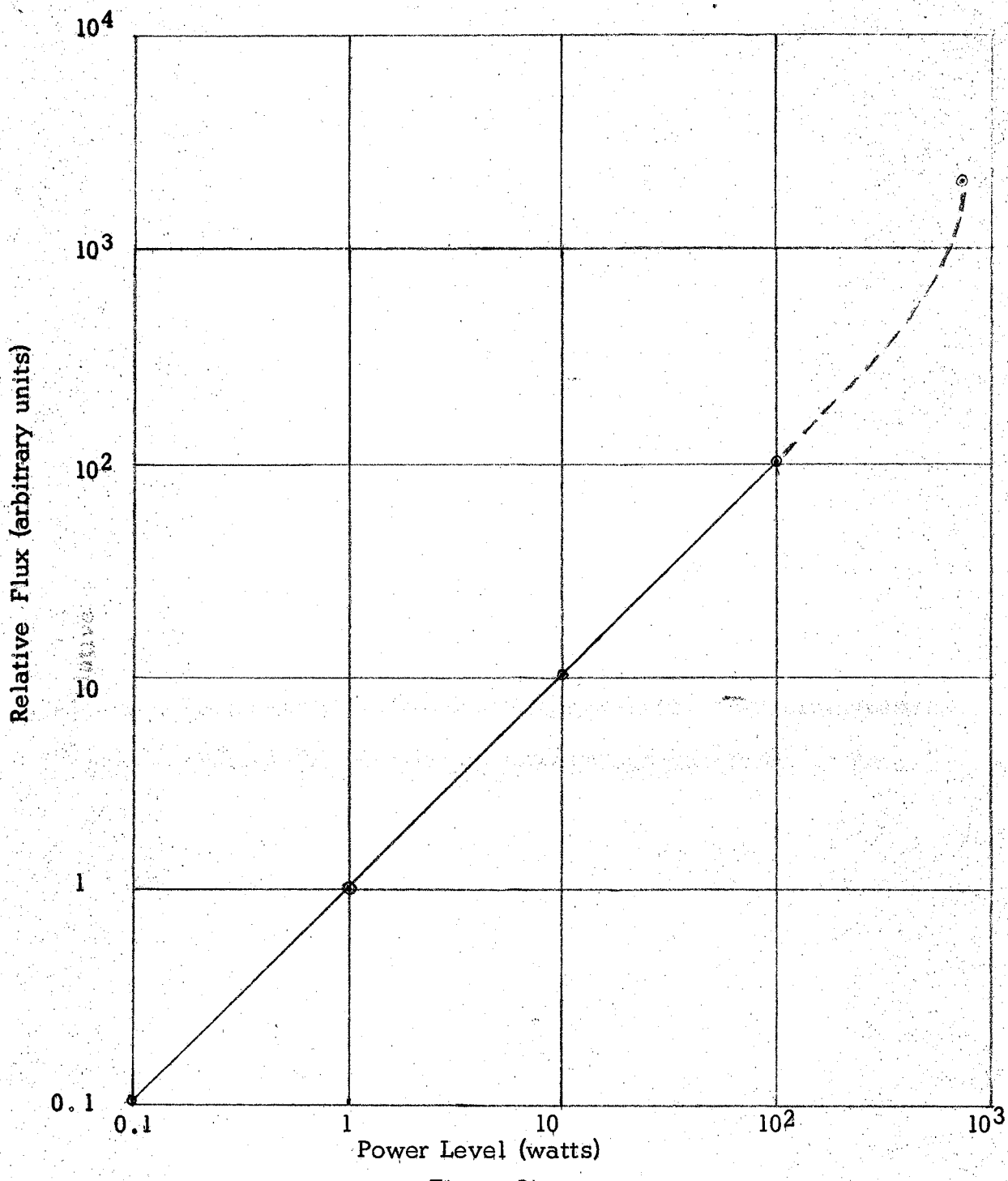


Figure 2

and not the result of random error. A possible reason may be that at powers above 100 watts enough epithermal neutrons reach the position of the indium foil to give a significant amount of activation from resonance capture.

7. Calculation of absolute neutron flux.

The number of events under the photopeak per unit time is related to the absolute gamma emission rate of the foil by the expression:

$$R_a = \frac{N_p}{R_{pt} \cdot E_t \cdot F_s \cdot F_{ic} \cdot F_a}$$

$N_p$ = total (computed) number of events under the photopeak

$R_{pt}$ = peak-to-total ratio (0.725)

$E_t$ = crystal detector efficiency (0.0846)

$F_s$ = correction for gamma self-absorption (0.997)

$F_{ic}$ = correction for internal conversion (0.96)

$F_a$ = correction for absorbing material in can (0.99)

The crystal efficiency was provided by Heath (9). The self-absorption expression was determined from the equation:

$$F_s = \frac{\mu t}{1 - e^{-\mu t}}$$

For gold foils 0.0005" thick, $\mu = 0.19$, and $t = 0.021$ g/cm$^2$; $F_s = 0.997$. $F_{ic}$ is given by Raffle (11) as 0.96. $F_a$ comes from the usual exponential attenuation formula, using $\mu = 0.0287$ for aluminum, and $t = 0.5$, from data furnished by Heath (9).

For determining the thermal flux from the disintegration rate, the

expression is:

$$\phi_{th} = \frac{R_a \cdot W \cdot F_\phi}{m \cdot N_o \cdot F_{fd} \cdot e^{-\lambda t} \cdot (1 - e^{-\lambda T}) \cdot \sigma a}$$

W = atomic mass of gold (197)

$F_\phi$ = ratio of thermal to total flux (0.815)

m = mass of sample

$N_o$ = Avogadro's number ($6.02 \times 10^{23}$)

$F_{fd}$ = flux depression correction (0.99)

$e^{-\lambda t}$ = correction for decay of sample

$1 - e^{-\lambda T}$ = activation factor

$\sigma a$ = effective cross section of sample (121.5 barns)

$F_\phi$ was calculated from the cadmium ratio of 5.36 determined by Kelly and Clements.

$F_{fd}$ was calculated for a 0.0005" foil by the method of Ritchie and Eldridge (12).

$\sigma a$ was calculated by applying the spectral hardening effect found by Cooke (3) to the procedure developed by Westcott (14) for deriving effective from thermal cross-sections. The basic expression is:

$$\sigma a = \sigma o \ (g + rs)$$

$\sigma a$ = effective cross-section (121.5 barns)

$\sigma o$ = thermal cross-section (98.8 barns)

g = non - 1/v factor (1.0053 at 20°C)

r = an expression relating thermal to total flux (0.013 for this reactor)

s = correction for resonance capture (17.3 at 20°C)

From the data in Westcott's paper and the cadmium ratio, r was calculated, and the values found used to determine the effective capture cross-section, which is higher than the thermal because of the large resonance correction for gold.

The results derived from the experimental data are presented in Table I, and a curve of flux versus nominal power is given in Figure 3.

TABLE I

| Power (watts) | Total flux ($_0n^1/cm^2/sec$) | Thermal flux ($_0n^1/cm^2/sec$) |
|---|---|---|
| 0.1 | $7.13 \times 10^6$ | $(5.81 \pm .12) \times 10^6$ |
| 0.1 | $7.29 \times 10^6$ | $(5.95 \pm .12) \times 10^6$ |
| 1 | $6.73 \times 10^7$ | $(5.48 \pm .11) \times 10^7$ |
| 1 | $7.02 \times 10^7$ | $(5.72 \pm .11) \times 10^7$ |
| 10 | $6.44 \times 10^8$ | $(5.25 \pm .10) \times 10^8$ |
| 10 | $6.41 \times 10^8$ | $(5.22 \pm .10) \times 10^8$ |
| 100 | $6.45 \times 10^9$ | $(5.26 \pm .10) \times 10^9$ |
| 100 | $6.50 \times 10^9$ | $(5.30 \pm .11) \times 10^9$ |
| 750 | $4.61 \times 10^{10}$ | $(3.75 \pm .08) \times 10^{10}$ |
| 750 | $4.70 \times 10^{10}$ | $(3.83 \pm .08) \times 10^{10}$ |

8. Discussion of results.

The values obtained for thermal flux are, in general, higher than those which have been previously reported. Kelly and Clements' figure for 0.1w was $5.31 \times 10^6$, while the value given by Copeland and Reasonover was $3.66 \times 10^6$, and Swanson (13) reported values of $5.09 \times 10^6$,

Absolute thermal flux vs. power level

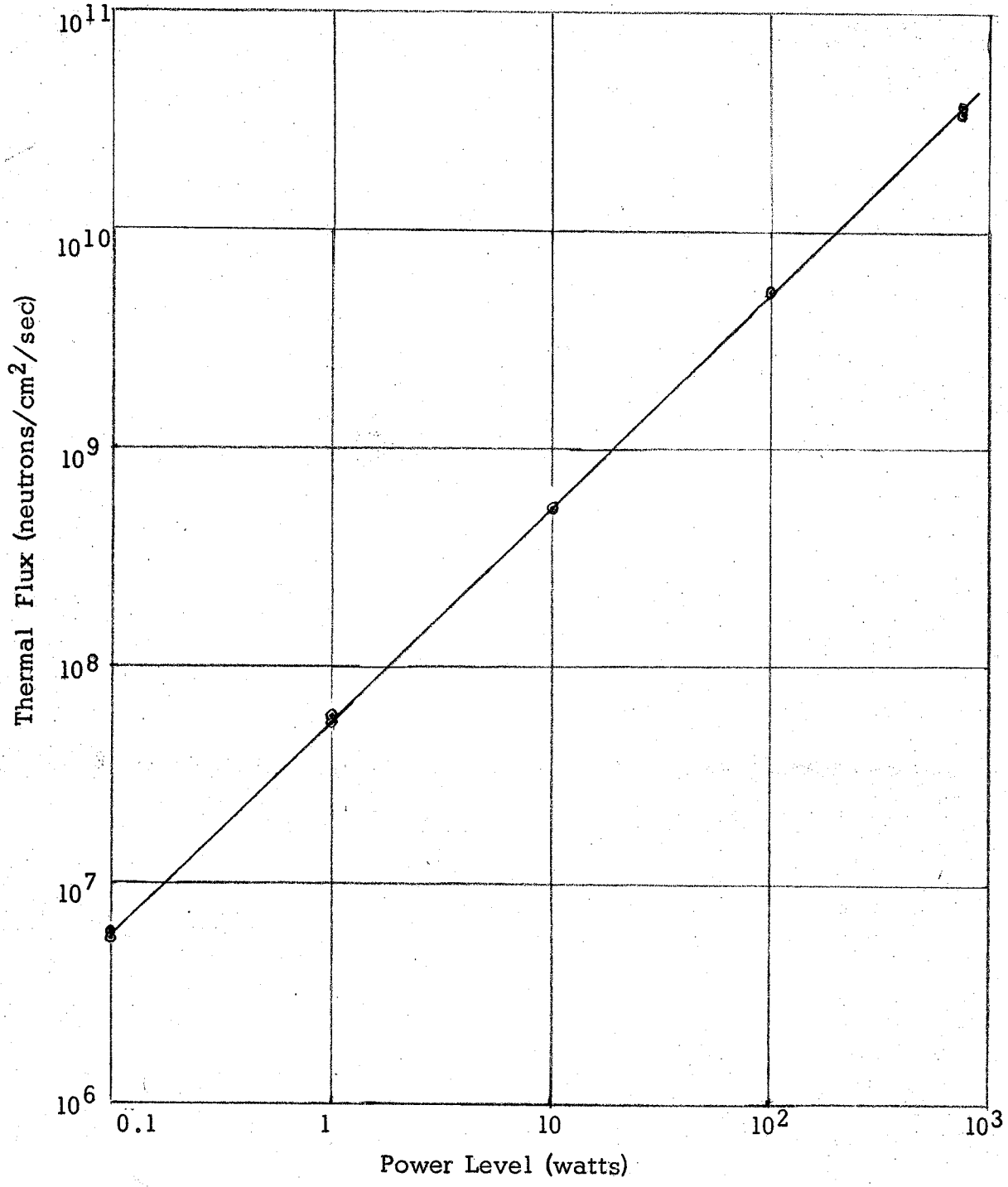


Figure 3

$4.84 \times 10^7$, and $4.32 \times 10^8$ for 0.1, 1, and 10 watts, respectively. His results are especially interesting, since they were obtained from good-geometry beta counting of indium foils after solution in HCl. A higher figure than that of Copeland and Reasonover is to be expected, since they were not aware of the crystal efficiency correction caused by the air gap in the crystal can; if their figure is adjusted to the correct efficiency, and also corrected for absorption, it becomes $5.11 \times 10^6$. It should also be noted that between 1961 and 1963 the physical location of the reactor instrumentation was changed. Although the two control channels affected were calibrated against each other before and after they were moved, there is a possibility that a particular indicated power level is now associated with a different flux.

The precision of the reported results is essentially that of the areas under the photopeaks. The average standard deviation of the means of all sets of areas taken was 2%; it is not considered justifiable to adjust this figure to reflect the exact deviation of a particular set of counts, since the deviations of all runs fell between 1% and 3%. The deviations listed in Table I are 2% of the reported flux values.

9. Summary

Thin gold foils were activated in the AGN-201 reactor, and their activation measured by gamma-ray scintillation spectrometry. Areas of photopeaks were individually computed by the CDC 1604 computer and averaged for each run, in order to minimize the effects of gain shift in the spectrometer. From the measured photopeak areas the total and thermal neutron fluxes were computed for power levels of 0.1, 1, 10, 100, and 750 watts. Flux values are given in Table I. They are somewhat

higher than the values obtained by previous investigators. Part of the difference arises from an incorrect value for crystal efficiency used in the earlier work.

I should like to acknowledge my gratitude and obligation to Professor William W. Hawes, of the Department of Metallurgy and Chemistry, for guidance, encouragement, and support throughout the progress of this investigation. Appreciation is also due to Harold L. McFarland, who kept the reactor "on course" for many hours; to Patricia C. Johnson, who prepared the computer program that is the heart of the calculations, and to Mr. R. L. Heath, of Phillips Petroleum Co., for crystal efficiency and other data.

## BIBLIOGRAPHY


1. Altekruse, E. B. A drift free gamma ray spectrometer for neutron radioactivation analysis. Thesis, U. S. Naval Postgraduate School, 1956.

2. Cantarell, I. Theoretical and experimental study of fatigue in photomultiplier tubes. Nuc. Sci. and Eng., 18:31, 1964.

3. Cooke, W. B. H. Predicted behaviour of the AGN-201 reactor at high power levels. Thesis, U. S. Naval Postgraduate School, 1961.

4. Copeland, E. C., and Reasonover, R. L., Jr. Investigation of thermal neutron flux perturbation in a polyethylene medium by use of gold foil detectors. Thesis, U. S. Naval Postgraduate School, 1961.

5. Covell, D. F., and Euler, B. A. Gain shift versus counting rate in certain multiplier phototubes. USNRDL-TR-521, U. S. Naval Radiological Defense Laboratory, June, 1961.

6. Ferguson, D. E., and Harvey, W. D. Determination of AGN-201 reactor operating parameters at high powers. Thesis, U.S. Naval Postgraduate School, 1963.

7. Heath, R. L. Scintillation spectrometry gamma-ray spectrum catalogue. Phillips Petroleum Co., Idaho Falls, Idaho, 1957.

8. Heath, R. L. Scintillation spectrometry handbook. Phillips Petroleum Co., Idaho Falls, Idaho, 1957.

9. Heath, R. L. Private communication, 1964.

10. Kelly, J. J., Jr., and Clements, N. W. Determination of thermal neutron flux by activation of a pure target with known cross section. Thesis, U. S. Naval Postgraduate School, 1960.

11. Raffle, J. F. Determination of absolute neutron flux by gold activation. J. Nuclear Energy, Part A: Reactor Science, vol. 10, 1959.

12. Ritchie, R. L., and Eldridge, H. B. Thermal neutron flux depression by absorbing foils. Nuc. Sci. and Eng., 8:300, 1960.

13. Swanson, C. A. L. Reactor thermal neutron flux measurements through proportional counting of dissolved, irradiated indium. Research paper, U. S. Naval Postgraduate School, 1963.

14. Westcott, C. H. Effective cross section values for well-moderated thermal reactor spectra. AECL-1101, Chalk River, Ontario, Canada, November, 1963.

## APPENDIX I

1. G-M coincidence correction.

For corrections which are not too large (less than 10% is the usual criterion), the relation of true sample activity, $\alpha$, to the observed activity, $\alpha'$, is given by:

$$\alpha' = \frac{\alpha}{1 + \tau\alpha}$$

where $\tau$ is the dead time of the Geiger-Muller tube. If the counting interval is chosen as unit time, the true and observed total counts, n and $n'$, can be substituted for the activities. In order to determine $\tau$, three samples of iodine were irradiated until the I-128 activity produced about 400 observed counts per second. Each sample was counted for one minute at six-minute intervals, until the activity had decayed to a level well below that for which a correction would be expected, but still high enough to give sufficient statistical precison. These lower counts were then corrected for decay back to earlier times, giving a series of computed "true" counts, $n_t$.

Substituting and rearranging in the equation above gives:

$$\tau = \frac{n_t - n'_t}{n_t\, n'_t}$$

The observed count for each of several times was used with the computed $n_t$ for each sample. Statistical variation in the counts, which is multiplied when the decay correction is applied, introduces variations in the computed value of $\tau$, but by taking enough values a good mean can be obtained. In the present case, seven values were chosen from each of three samples. Values for $\tau$ computed from the first few counts are not

usable, either because the coincidence correction is greater than 10% or because the resolution time of the scaler becomes important, but with a column of computed values it is easy to see the point at which they settle down around a steady mean. A similar precaution applies to using counts below the middle range. If the statistical variation of $n'_t$ is too great, $\tau$ will be unreliable.

2. Initial activity from integrated counts.

In the present work, the purpose of counting the indium foils was to determine their activity, $\alpha_o$, at the time of removal from the reactor. In order to have the best precision, it was desirable to count the sample over a fairly long period of time -- 10 minutes was chosen -- but with its 54-minute half-life, In-116 decays significantly in 10 minutes, and both the activity and the coincidence correction change, at different rates, between the beginning and end of the count. The following derivation enables one to calculate $\alpha_o$ directly from an integrated count taken over any period.

Let

$\alpha$ = true activity at any time.

$\alpha'$ = observed activity at any time.

$\alpha_o$ = desired activity at time $t_o$.

$\alpha_i$ = activity at start of count.

$t_1$ = time from $t_o$ to start of count.

T = length of count.

$\tau$ = G-M dead time.

n = true integrated count in time T.

$n'$ = observed integrated count in time T.

By definition,

$$n = \int_0^T \alpha \, dt$$

And

$$n' = \int_0^T \alpha' \, dt = \int_0^T \frac{\alpha}{1 + \tau\alpha} \, dt$$

$$\frac{\alpha \, dt}{1 + \tau\alpha} = \frac{\left(\frac{\alpha_i}{e^{\lambda t}}\right) dt}{1 + \tau \frac{\alpha_i}{e^{\lambda t}}} = \frac{\alpha_i \, dt}{\tau\alpha_i + e^{\lambda t}}$$

$$\int_0^T \frac{\alpha}{1 + \tau\alpha} \, dt = \alpha_i \int_0^T \frac{dt}{\tau\alpha_i + e^{\lambda t}}$$

$$n' = \alpha_i \left[ \frac{t}{\alpha_i \tau} - \frac{1}{\alpha_i \lambda \tau} \ln (\alpha_i \tau + e^{\lambda t}) \right]_0^T$$

$$n' = \frac{T}{\tau} - \frac{1}{\lambda\tau} \ln (\alpha_i \tau + e^{\lambda T}) + \frac{1}{\lambda\tau} \ln (\alpha_i \tau + 1)$$

$$n' = \frac{T}{\tau} + \frac{1}{\lambda\tau} \ln \frac{\alpha_i \tau + 1}{\alpha_i \tau + e^{\lambda T}}$$

Then $$\ln \frac{\alpha_i \tau + 1}{\alpha_i \tau + e^{\lambda T}} = \left( n' - \frac{T}{\tau} \right) \lambda\tau = n' \lambda\tau - \lambda T$$

In exponential form,

$$\frac{\alpha_i \tau + 1}{\alpha_i \tau + e^{\lambda T}} = e^{n'\lambda\tau - \lambda T} = e^{n'\lambda\tau} \times e^{-\lambda T}$$

Solving for $\alpha_i$,

$$\alpha_i = \frac{e^{n'\lambda\tau} - 1}{\tau(1 - e^{n'\lambda\tau} \times e^{-\lambda T})}$$

From which

$$\alpha_o = \frac{(e^{n'\lambda\tau} - 1)\, e^{\lambda t}}{(1 - e^{n'\lambda\tau - \lambda T})}$$

## APPENDIX II

## EXPERIMENTAL DATA

Experimental points used in determining photopeak areas are given below. Each set of four points represents one complete count over the photopeak; all counts were one minute long. Values given are corrected back to the time of removal from the reactor.

0.1 watt Run 1
Mass; 30.0 mg
Irradiation time 477.7 min.

| | Channel | Count |
|---|---|---|
| 1. | 19 | 3020 |
| | 20 | 2778 |
| | 21 | 1769 |
| | 22 | 1038 |
| 2. | 19 | 2993 |
| | 20 | 2917 |
| | 21 | 1729 |
| | 22 | 1136 |
| 3. | 19 | 3496 |
| | 20 | 2889 |
| | 21 | 1625 |
| | 22 | 752 |
| 4. | 19 | 3103 |
| | 20 | 2759 |
| | 21 | 1510 |
| | 22 | 936 |
| 5. | 19 | 3093 |
| | 20 | 2710 |
| | 21 | 1676 |
| | 22 | 832 |
| 6. | 19 | 3119 |
| | 20 | 2732 |
| | 21 | 1540 |
| | 22 | 855 |
| 7. | 19 | 3107 |
| | 20 | 2707 |
| | 21 | 1801 |
| | 22 | 875 |
| 8. | 19 | 3050 |
| | 20 | 2790 |
| | 21 | 1776 |
| | 22 | 951 |

0.1 watt Run 2
Mass: 31.5 mg
Irradiation time 534 min.

| | | |
|---|---|---|
| 1. | 19 | 5161 |
| | 20 | 5408 |
| | 21 | 4191 |
| | 22 | 2617 |
| 2. | 19 | 5030 |
| | 20 | 5426 |
| | 21 | 4069 |
| | 22 | 2443 |
| 3. | 19 | 5337 |
| | 20 | 5315 |
| | 21 | 3628 |
| | 22 | 2318 |
| 4. | 19 | 5065 |
| | 20 | 5343 |
| | 21 | 3670 |
| | 22 | 2407 |

0.1 watt Run 2 (continued)

| | Channel | Count |
|---|---|---|
| 5. | 19 | 5016 |
| | 20 | 5280 |
| | 21 | 4088 |
| | 22 | 2545 |
| 6. | 19 | 5071 |
| | 20 | 5204 |
| | 21 | 4181 |
| | 22 | 2472 |

1 watt Run 1
Mass: 31.0 mg
Irradiation time 60 min.

| | Channel | Count |
|---|---|---|
| 1. | 23 | 5833 |
| | 24 | 5340 |
| | 25 | 3798 |
| | 26 | 1686 |
| 2. | 23 | 5861 |
| | 24 | 5033 |
| | 25 | 3379 |
| | 26 | 1711 |
| 3. | 23 | 5766 |
| | 24 | 5187 |
| | 25 | 3493 |
| | 26 | 1831 |
| 4. | 23 | 5965 |
| | 24 | 5020 |
| | 25 | 3596 |
| | 26 | 1782 |
| 5. | 23 | 6016 |
| | 24 | 4623 |
| | 25 | 3498 |
| | 26 | 1577 |
| 6. | 23 | 5855 |
| | 24 | 4961 |
| | 25 | 3027 |
| | 26 | 1368 |
| 7. | 22 | 5276 |
| | 23 | 5873 |
| | 24 | 4604 |
| | 25 | 3043 |
| 8. | 22 | 5844 |
| | 23 | 5631 |
| | 24 | 3957 |
| | 25 | 2255 |
| 9. | 22 | 5633 |
| | 23 | 5647 |
| | 24 | 4092 |
| | 25 | 2500 |
| 10. | 22 | 5725 |
| | 23 | 5499 |
| | 24 | 4588 |
| | 25 | 2997 |
| 11. | 22 | 5736 |
| | 23 | 5678 |
| | 24 | 4514 |
| | 25 | 2300 |

1 watt Run 2
Mass: 29.5 mg
Irradiation time 60 min.

| | Channel | Count |
|---|---|---|
| 1. | 22 | 5204 |
| | 23 | 5359 |
| | 24 | 4098 |
| | 25 | 2620 |
| 2. | 22 | 5349 |
| | 23 | 5498 |
| | 24 | 4347 |
| | 25 | 2493 |
| 3. | 22 | 5420 |
| | 23 | 5441 |
| | 24 | 4081 |
| | 25 | 2499 |
| 4. | 22 | 5479 |
| | 23 | 5522 |
| | 24 | 4348 |
| | 25 | 2550 |
| 5. | 22 | 5370 |
| | 23 | 5295 |
| | 24 | 3902 |
| | 25 | 2397 |
| 6. | 22 | 5444 |
| | 23 | 5419 |
| | 24 | 4333 |
| | 25 | 2509 |
| 7. | 22 | 5511 |
| | 23 | 5478 |
| | 24 | 3222 |
| | 25 | 2172 |
| 8. | 22 | 5590 |
| | 23 | 5374 |
| | 24 | 3744 |
| | 25 | 2276 |

10 watt Run 1
Mass: 28.5 mg
Irradiation time 30 min.

| | | |
|---|---|---|
| 1. | 21 | 26739 |
| | 22 | 23023 |
| | 23 | 14933 |
| | 24 | 6933 |
| 2. | 21 | 26929 |
| | 22 | 22080 |
| | 23 | 15087 |
| | 24 | 7952 |
| 3. | 21 | 26433 |
| | 22 | 23422 |
| | 23 | 15435 |
| | 24 | 8062 |
| 4. | 21 | 26611 |
| | 22 | 24276 |
| | 23 | 16989 |
| | 24 | 9220 |
| 5. | 21 | 25863 |
| | 22 | 24564 |
| | 23 | 17573 |
| | 24 | 9287 |
| 6. | 21 | 25665 |
| | 22 | 24161 |
| | 23 | 16943 |
| | 24 | 9131 |
| 7. | 21 | 25536 |
| | 22 | 24034 |
| | 23 | 16711 |
| | 24 | 9491 |
| 8. | 21 | 25144 |
| | 22 | 23927 |
| | 23 | 16624 |
| | 24 | 8849 |
| 9. | 21 | 26477 |
| | 22 | 23615 |
| | 23 | 16310 |
| | 24 | 6373 |

10 watts Run 2
Mass: 30.0 mg
Irradiation time 30 min.

| | Channel | Count | | Channel | Count |
|---|---|---|---|---|---|
| 1. | 21 | 27346 | 5. | 21 | 27427 |
| | 22 | 24734 | | 22 | 24370 |
| | 23 | 17311 | | 23 | 16329 |
| | 24 | 7871 | | 24 | 8544 |
| 2. | 21 | 27110 | 6. | 21 | 27886 |
| | 22 | 24814 | | 22 | 23827 |
| | 23 | 17601 | | 23 | 15840 |
| | 24 | 9104 | | 24 | 7741 |
| 3. | 21 | 27999 | 7. | 21 | 27982 |
| | 22 | 24786 | | 22 | 24177 |
| | 23 | 16980 | | 23 | 16002 |
| | 24 | 8022 | | 24 | 7915 |
| 4. | 21 | 27271 | 8. | 21 | 27862 |
| | 22 | 24834 | | 22 | 23279 |
| | 23 | 16740 | | 23 | 15290 |
| | 24 | 9071 | | 24 | 7799 |

100 watts Run 1
Mass: 29.0 mg
Irradiation time 10 min.

| | | | | | |
|---|---|---|---|---|---|
| 1. | 20 | 90328 | 6. | 20 | 90152 |
| | 21 | 79321 | | 21 | 78586 |
| | 22 | 54308 | | 22 | 53088 |
| | 23 | 25996 | | 23 | 25587 |
| 2. | 20 | 92303 | 7. | 20 | 85047 |
| | 21 | 82679 | | 21 | 85918 |
| | 22 | 50305 | | 22 | 65734 |
| | 23 | 24699 | | 23 | 38091 |
| 3. | 20 | 89959 | 8. | 20 | 86027 |
| | 21 | 80298 | | 21 | 86495 |
| | 22 | 54834 | | 22 | 62329 |
| | 23 | 27463 | | 23 | 33931 |
| 4. | 20 | 91006 | 9. | 20 | 89215 |
| | 21 | 74540 | | 21 | 83291 |
| | 22 | 45774 | | 22 | 58807 |
| | 23 | 21665 | | 23 | 32023 |
| 5. | 20 | 89693 | 10. | 20 | 90518 |
| | 21 | 79115 | | 21 | 79197 |
| | 22 | 52516 | | 22 | 51580 |
| | 23 | 27593 | | 23 | 26720 |

100 watts Run 2
Mass: 31.0 mg
Irradiation time 10 min.

| | Channel | Count | | Channel | Count |
|---|---|---|---|---|---|
| 1. | 20 | 97092 | 6. | 20 | 97500 |
| | 21 | 83991 | | 21 | 86819 |
| | 22 | 57262 | | 22 | 57588 |
| | 23 | 29511 | | 23 | 28592 |
| 2. | 20 | 95656 | 7. | 20 | 95811 |
| | 21 | 82661 | | 21 | 85773 |
| | 22 | 53035 | | 22 | 59232 |
| | 23 | 27731 | | 23 | 27300 |
| 3. | 20 | 96532 | 8. | 20 | 97178 |
| | 21 | 81315 | | 21 | 84094 |
| | 22 | 53139 | | 22 | 57617 |
| | 23 | 24804 | | 23 | 30875 |
| 4. | 20 | 95844 | 9. | 20 | 95279 |
| | 21 | 84405 | | 21 | 89158 |
| | 22 | 55160 | | 22 | 60150 |
| | 23 | 28091 | | 23 | 30561 |
| 5. | 20 | 96219 | | | |
| | 21 | 80541 | | | |
| | 22 | 54445 | | | |
| | 23 | 25940 | | | |

750 watts Run 1
Mass: 30.0 mg
Irradiation time 5 min.

| | | | | | |
|---|---|---|---|---|---|
| 1. | 23 | 361,355 | 5. | 23 | 353,481 |
| | 24 | 316,663 | | 24 | 301,519 |
| | 25 | 206,301 | | 25 | 186,786 |
| | 26 | 92152 | | 26 | 80748 |
| 2. | 23 | 360,305 | 6. | 23 | 360,133 |
| | 24 | 303,361 | | 24 | 300,968 |
| | 25 | 202,571 | | 25 | 197,930 |
| | 26 | 91250 | | 26 | 91893 |
| 3. | 23 | 358,049 | 7. | 23 | 363,002 |
| | 24 | 306,995 | | 24 | 316,068 |
| | 25 | 200,594 | | 25 | 210,761 |
| | 26 | 88118 | | 26 | 93839 |
| 4. | 23 | 350,035 | | | |
| | 24 | 293,764 | | | |
| | 25 | 186,034 | | | |
| | 26 | 77688 | | | |

750 watts
Mass:
Irradiation time

Run 2
32.0 mg
5 min.

| | Channel | Count |
|---|---|---|
| 1. | 23 | 387,878 |
| | 24 | 342,060 |
| | 25 | 222,754 |
| | 26 | 105,531 |
| 2. | 23 | 383,478 |
| | 24 | 340,082 |
| | 25 | 212,931 |
| | 26 | 99094 |
| 3. | 23 | 387,472 |
| | 24 | 335,694 |
| | 25 | 208,157 |
| | 26 | 96726 |
| 4. | 23 | 381,343 |
| | 24 | 359,159 |
| | 25 | 221,929 |
| | 26 | 101,741 |
| 5. | 23 | 392,784 |
| | 24 | 341,144 |
| | 25 | 216,476 |
| | 26 | 102,292 |

## APPENDIX III

## PHOTOPEAK PARAMETERS

| Foil | Count | Abscissa of maximum | Ordinate of maximum | Area |
|---|---|---|---|---|
| 0.1 w, Run 1 | 1. | 18.93 | 4969 | 25753 |
| | 2. | 18.91 | 4992 | 26860 |
| | 3. | 18.76 | 5772 | 26513 |
| | 4. | 18.43 | 5340 | 29662 |
| | 5. | 18.97 | 5052 | 23569 |
| | 6. | 18.67 | 5223 | 26492 |
| | 7. | 19.05 | 5041 | 23438 |
| | 8. | 19.06 | 4997 | 23926 |
| | | | Average | 25777 ± 745 |
| 0.1 w, Run 2 | 1. | 19.66 | 5478 | 26021 |
| | 2. | 19.60 | 5358 | 26082 |
| | 3. | 19.21 | 5448 | 28919 |
| | 4. | 19.42 | 5273 | 26890 |
| | 5. | 19.62 | 5301 | 26104 |
| | 6. | 19.62 | 5335 | 25812 |
| | | | Average | 26638 ± 480 |
| 1 w, Run 1 | 1. | 23.36 | 5913 | 24872 |
| | 2. | 22.94 | 5855 | 28620 |
| | 3. | 23.08 | 5781 | 27824 |
| | 4. | 22.97 | 5915 | 29148 |
| | 5. | 22.81 | 5924 | 29585 |
| | 6. | 22.96 | 5863 | 26170 |
| | 7. | 22.78 | 5765 | 28144 |
| | 8. | 22.29 | 5937 | 28885 |
| | 9. | 22.40 | 5787 | 28942 |
| | 10. | 22.39 | 5782 | 33146 |
| | 11. | 22.60 | 6017 | 26367 |
| | | | Average | 28337 ± 592 |
| 1 w, Run 2 | 1. | 22.53 | 5413 | 27661 |
| | 2. | 22.63 | 5653 | 26287 |
| | 3. | 22.45 | 5581 | 28033 |
| | 4. | 22.56 | 5705 | 27530 |
| | 5. | 22.36 | 5480 | 28094 |
| | 6. | 22.55 | 5647 | 27295 |
| | 7. | 21.95 | 5671 | 30622 |
| | 8. | 22.19 | 5660 | 29330 |
| | | | Average | 28107 ± 469 |

| Foil | Count | Abscissa of maximum | Ordinate of maximum | Area |
|---|---|---|---|---|
| 10 w, Run 1 | 1. | 21.04 | 26692 | 120,798 |
| | 2. | 20.65 | 27201 | 145,846 |
| | 3. | 21.01 | 26504 | 128,677 |
| | 4. | 21.14 | 26691 | 131,213 |
| | 5. | 21.34 | 26271 | 121,741 |
| | 6. | 21.26 | 25952 | 122,990 |
| | 7. | 21.19 | 25769 | 127,843 |
| | 8. | 21.30 | 25532 | 118,468 |
| | 9. | 21.35 | 26788 | 105,950 |
| | | | Average | 124,836 ± 3599 |
| 10 w, Run 2 | 1. | 21.29 | 27545 | 118,689 |
| | 2. | 21.23 | 27236 | 128,184 |
| | 3. | 21.17 | 27993 | 125,965 |
| | 4. | 21.09 | 27394 | 134,143 |
| | 5. | 21.03 | 27471 | 133,548 |
| | 6. | 20.97 | 28103 | 140,952 |
| | 7. | 20.99 | 27954 | 132,878 |
| | 8. | 20.78 | 28016 | 141,493 |
| | | | Average | 130,914 ± 2378 |
| 100 w, Run 1 | 1. | 20.13 | 90149 | 412,613 |
| | 2. | 20.05 | 92989 | 420,643 |
| | 3. | 20.13 | 90021 | 420,746 |
| | 4. | 19.76 | 91841 | 438,778 |
| | 5. | 19.98 | 89884 | 441,322 |
| | 6. | 20.08 | 89932 | 416,033 |
| | 7. | 20.54 | 88519 | 420,892 |
| | 8. | 20.49 | 89438 | 403,893 |
| | 9. | 20.23 | 89946 | 433,832 |
| | 10. | 19.95 | 90793 | 442,734 |
| | | | Average | 425,149 ± 4192 |
| 100 w, Run 2 | 1. | 19.97 | 96940 | 478,690 |
| | 2. | 19.86 | 96248 | 478,386 |
| | 3. | 19.96 | 96233 | 446,182 |
| | 4. | 20.01 | 96038 | 458,672 |
| | 5. | 19.94 | 95733 | 455,721 |
| | 6. | 20.10 | 97662 | 452,845 |
| | 7. | 20.24 | 96128 | 421,151 |
| | 8. | 19.90 | 97235 | 498,277 |
| | 9. | 20.26 | 96441 | 436,508 |
| | | | Average | 458,492 ± 7866 |

| Foil | Count | Abscissa of maximum | Ordinate of maximum | Area |
|---|---|---|---|---|
| 750 w, Run 1 | 1. | 23.15 | 361,455 | 1,567,600 |
| | 2. | 23.03 | 358,013 | 1,619,320 |
| | 3. | 23.10 | 356,814 | 1,557,260 |
| | 4. | 23.06 | 348,365 | 1,489,360 |
| | 5. | 23.05 | 353,070 | 1,521,690 |
| | 6. | 22.95 | 358,724 | 1,669,420 |
| | 7. | 23.15 | 362,365 | 1,579,730 |
| | | | Average | 1,572,050 ± 22570 |
| 750 w, Run 2 | 1. | 23.10 | 388,279 | 1,747,580 |
| | 2. | 23.10 | 384,938 | 1,694,390 |
| | 3. | 23.01 | 388,204 | 1,738,740 |
| | 4. | 23.28 | 388,743 | 1,613,890 |
| | 5. | 23.03 | 393,131 | 1,784,240 |
| | | | Average | 1,715,770 ± 29210 |